NIH Public Access
Author Manuscript
Structure. Author manuscript; available in PMC 2011 October 13.

Published in final edited form as:
Structure. 2010 October 13; 18(10): 1311–1320. doi:10.1016/j.str.2010.07.010.

Structural analysis of the interaction between Dishevelled2 and clathrin AP-2 adaptor, a critical step in non-canonical Wnt signaling

Anan Yu[1,*], **Yi Xing**[2,*], **Stephen C. Harrison**[2,3], and **Tomas Kirchhausen**[1]

[1] Department of Cell Biology and Immune Disease Institute, Harvard Medical School, Boston, MA 02115

[2] Jack and Eileen Connors Structural Biology Laboratory, Department of Biological Chemistry and Molecular Pharmacology, Harvard Medical School, Boston, MA 02115

[3] Howard Hughes Medical Institute

Abstract

Wnt association with its receptor, Frizzled (Fz), and recruitment by the latter of an adaptor, Dishevelled (Dvl), initiates signaling through at least two distinct pathways ("canonical" and "non-canonical"). Endocytosis and compartmentalization help determine the signaling outcome. Our previous work has shown that Dvl2 links at least one Frizzled family member (Fz4) to clathrin-mediated endocytosis by interacting with the μ2 subunit of the AP-2 clathrin adaptor, through both a classical endocytic tyrosine motif and a so-called "DEP domain". We report here the crystal structure of a chimeric protein that mimics the Dvl2-μ2 complex. The DEP domain binds at one end of the elongated, C-terminal domain of μ2. This domain:domain interface shows that parts of the μ2 surface distinct from the tyrosine-motif site can help recruit specific receptors or adaptors into a clathrin coated pit. Mutation of residues at the DEP-μ2 contact or in the tyrosine motif reduce affinity of Dvl2 for μ2 and block efficient internalization of Fz4 in response to ligation by Wnt5a. The crystal structure has thus allowed us to identify the specific interaction that leads to Frizzled uptake and to downstream, non-canonical signaling events.

Wnt signaling regulates a number of major developmental events, through at least two classes of pathways (Kikuchi et al., 2009; Logan and Nusse, 2004; Veeman et al., 2003; Wallingford and Habas, 2005; Wehrli and Tomlinson, 1998). Both begin with binding of a Wnt-family ligand to its membrane receptor, Frizzled (Fz), in some cases together with co-receptors such as a low-density lipoprotein receptor-related protein 6 (LRP6) or receptor tyrosine kinases. Frizzled (Fz) can recruit cytosolic adaptors, such as Dishevelled (Dvl), which in turn interact with downstream effectors. Wnt, Frizzled, and Dishevelled all represent families of related molecules, leading to a complex diversity of signaling outcomes.

Endocytosis and compartmentalization of Wnt ligands and their receptors and co-receptors help determine the signaling outcome (Chen et al., 2003; Sato et al., 2010; Yu et al., 2007). There is good evidence for selective activation in endosomal compartments of specific branches of Wnt-determined signaling (Blitzer and Nusse, 2006; Dubois et al., 2001; Piddini et al., 2005; Rives et al., 2006; Sato et al., 2010; Seto and Bellen, 2006; Yu et al., 2007).

Corresponding author: Tomas Kirchhausen, Harvard Medical School/IDI, 200 Longwood Ave, Boston MA 02115, Phone: 617.713.8888, FAX: 617.713.8898, kirchhausen@crystal.harvard.edu.

*Equal contribution

NIH-PA Author Manuscript
NIH-PA Author Manuscript
NIH-PA Author Manuscript

NIH-PA Author Manuscript

NIH-PA Author Manuscript

NIH-PA Author Manuscript

Compartmentalization probably also fine tunes signaling strength by removing activated receptors from the cell surface and by terminating signaling activity through lysosomal degradation.

Wnt binding to Frizzled, a seven-transmembrane helix protein, and to LRP6, its co-receptor, induces through Dishevelled a signaling cascade known as the “canonical” pathway (He et al., 2004; Tamai et al., 2000; Wehrli et al., 2000). This pathway stabilizes cytosolic β-catenin and leads to gene-specific transcriptional activation. Fz-Dvl complexes also induce a β-catenin independent class of signaling cascades -- the “non-canonical” Wnt pathway -- by activating the small GTPases RhoA, Rac, and Cdc42 (Boutros and Mlodzik, 1999; Eaton and Simons, 1995; Fanto et al., 2000; Sato et al., 2010). Non-canonical Wnt signaling regulates cytoskeletal reorganization, cell movement, and planar cell polarity (PCP). Its specificity depends on the pairing of particular Wnt ligands with particular Fz family members (e.g., Wnt5A and Fz4). Our previous work (Yu et al., 2007) provides strong evidence that clathrin-mediated endocytosis of Fz4 is necessary to activate non-canonical signaling and that Dvl2 links the relevant Fz receptor to the clathrin endocytic apparatus through an interaction with the endocytic AP-2 clathrin adaptor. A recent study has confirmed this observation by showing that Wnt5a-dependent activation of Rac requires clathrin-mediated internalization of Fz2 (Sato et al., 2010).

AP-2 is a heterotetramer (α,β2,μ2,σ2) that links the clathrin coat to the cargo proteins and membrane lipids of the coated vesicle (Kirchhausen, 1999; Owen et al., 2004). The μ2 subunit recognizes tyrosine sorting motifs in the cytosolic tails of various membrane proteins and draws these proteins (and their extracellular ligands) into assembling coated pits. We showed in a genome-wide, yeast-two-hybrid screen, confirmed by immunoprecipitation and pull-down assays, that Dvl2 and μ2 interact and that the interaction is essential for the non-canonical pathway (Yu et al., 2007). Association of Dvl2 and μ2 requires a classical endocytic tyrosine motif in Dvl2 as well as its “DEP domain” (a ~90-residue domain, named after Dishevelled, Egl-10, and Pleckstrin, the proteins in which it was first identified). Single point mutations in the tyrosine motif that affect the Dvl2:μ2 interaction compromise non-canonical Wnt signaling both in isolated cells and in developing *Xenopus* embryos, whereas the Dvl2-μ2 association does not appear to affect canonical Wnt signaling (Yu et al., 2007). Thus, a point mutation that alters endocytic trafficking of the receptor has revealed distinct signaling outcomes for the same molecule at different intracellular locations (plasma membrane vs. endosomes). We postulated that trafficking of Wnt/Fz complexes to endosomes is essential for activating non-canonical downstream targets. Because Dvl2 can bind β-arrestin2, it has been proposed that the latter molecule mediates Fz4 internalization indirectly, through its own contacts with AP-2 and clathrin (Chen et al., 2003); our results demonstrating that a direct μ2-Dvl2 contact is required for Fz4 uptake argues against a primary role for β-arrestin2 in directing Fz4 endocytosis.

In the work reported here, we have determined the crystal structure of a chimeric protein that mimics the Dvl2-μ2 complex. It includes the two elements from Dvl2 that we have shown participate in μ2 association: the DEP domain and the tyrosine motif (YHEL). The tyrosine motif binds the C-terminal domain of μ2 (μ2C) at a well-characterized location (Owen and Evans, 1998); the DEP domain binds at one end of the elongated μ2C, docking against a surface that would be exposed even on intact AP-2 (Collins et al., 2002). Mutations, in the tyrosine motif or in its pocket on μ2 or at the DEP-μ2C interface, diminish the affinity of Dvl2 for μ2C. Overexpression of Dvl2 mutants with a compromised DEP:μ2 interaction prevent efficient internalization of Fz4 stimulated by Wnt5a. These results show that the crystal structure has led to identification of the specific interaction that determines Fz4 endocytosis and downstream non-canonical signaling events.

NIH-PA Author Manuscript

NIH-PA Author Manuscript

NIH-PA Author Manuscript

Results

Structure determination

Truncated forms of murine Dvl2, containing both the DEP domain and the tyrosine motif (YHEL), associate tightly with the C-terminal domain of μ2 (residues 170–435, here designated μ2C)((Yu et al., 2007) and Fig. S1A). The 60-residue, proline-rich linker segment connecting these two required elements are likely to be unstructured and flexible. We tested a series of deletions and found that a linker of just 11 residues was sufficient for strong binding (Fig. S1A). When even this form failed to yield crystals of a complex with μ2C, we constructed a set of single-chain chimeras, with a variable linker between DEP and YHEL and a second variable linker between YHEL and the N-terminus of μ2C. Optimization yielded well-ordered crystals of a chimeric protein with linkers of 11 and 8 residues, respectively. This species is a well-behaved monomer in solution (Fig. S1B,C).

We determined the structure by molecular replacement from diffraction data extending to a minimum Bragg spacing of 3.5 Å (see Methods). The space group is C2, with an asymmetric unit that contains 6 polypeptide chains. The packing is such that the tyrosine motif of one chain interacts with its binding site on μ2C of another chain, related to the former by a non-crystallographic twofold, generating a domain-swapped dimer (Fig. 1). The only remaining crystallographic contacts are between DEP domains and μ2C (Fig. 1A). One of these, which we identify experimentally as the functional interaction (see below), is substantially more extensive than the other; the buried surface areas are approximately 1540 $Å^2$ and 1000 $Å^2$, respectively. The μ2C and Dvl2 elements in our crystals correspond to the protein from rat, but the interface of Dvl2 and μ2C is identical in mouse and man and highly conserved in Xenopus (Fig. 2).

The Dvl2 DEP domain

The DEP domain is a 90-residue module with three α-helices packed against a small, sharply twisted, 4-stranded β-sheet (Fig. 1B,C; Fig. 2). The loop between strands β1 and β2 is an independent β-ribbon (β1′–β2′). The solution structure of the murine DEP domain, determined by nuclear magnetic resonance (NMR) spectroscopy (Wong et al., 2000), superposes well on our x-ray structure, except for the β1′–β2′ ribbon, which projects at an angle of almost 90° to its direction in the μ2C complex, displacing the tip by about 15 Å. No contacts within the DEP domain need to change in this shift; contacts with μ2C probably determine the new direction of the ribbon.

The DEP:μ2C interface

The μ2C domain is a gently curved banana-shaped slab, about 80 Å long, 30 Å wide, and less than 20 Å thick. The two crystallographically distinct DEP:μ2C contacts are at opposite ends of this elongated structure. Only the more extensive of the two is close enough to the tyrosine-motif site that an 11-residue linker could connect them. This contact covers nearly the entire surface of one narrow end of the μ2C slab. Principal DEP-domain contributions come from the N-terminal helix (α1), the β1′-β2′ ribbon, and strands β3 and β4 of the sheet (Fig. 3). A hydrophobic patch, containing DEP-domain residues Ile447, Ile449, Pro450 (all in the β1′-β2′ ribbon) and Val504, faces μ2C residues Phe407 and Pro409; Arg489 of the DEP domain, anchored by interaction with carbonyl 505, bridges to Glu211 (buttressed in turn by Arg253) and carbonyl 209 of μ2C; and DEP domain residues Asp441 and Asn451 bridge to μ2C lysines 213 and 405.

The μ2C surface covered by the DEP domain is fully exposed in the intact AP-2 core (PDB ID: 2VGL (Collins et al., 2002)), and we can dock the DEP domain onto the AP-2 core without molecular collisions (Fig. 4). The μ-chain hinge, joining its N- and C-terminal

NIH-PA Author Manuscript

NIH-PA Author Manuscript

NIH-PA Author Manuscript

domains, is a 20-residue, flexible segment, disordered in the AP-2 core structure, that would pass across the same μ2C surface, but the length and endpoints of the hinge would allow it to avoid the DEP contact completely. To dock the tyrosine motif, μ2C must shift away from the rest of the AP-2 core, as pointed out in the original analysis of an AP-2 crystal structure (Collins et al., 2002).

Influence of mutations at the DEP:μ2C interface on association of these proteins in vitro

We tested the influence of a set of mutations in μ2C on its association with Dvl2(407–588), a fragment that contains the DEP domain, the native linker and the YHEL motif. GST-μ2C variants, expressed in *E. coli*, were incubated with His-tagged Dvl2(407–588), and the components retained by a glutathione matrix were analyzed by SDS-PAGE, with Coomassie blue staining to detect GST-containing species and immunoblotting with an anti-His tag antibody to detect Dvl2. Mutation to alanine of each of four interface residues (Glu211, Lys213, Lys405, and Phe407) had only small effects individually but somewhat larger effects in various combinations. Mutations in the tyrosine-motif binding pocket had stronger effects. Thus, the stability of the complex in free solution depends on a combination of the two interactions, with the tyrosine-pocket interaction making the greater contribution. These data are consistent with our observation that the DEP domain alone does not co-migrate with μ2C when subjected to size-exclusion chromatography, whereas a fragment (residues 508–588) that lacks DEP but bears the YHEL motif does co-migrate (not shown). To demonstrate that the mutated μ2C species are properly folded, we tested the binding of a short peptide containing the YQRL motif from TGN38, an integral membrane protein in the trans Golgi network (Fig. 5) (Boll et al., 1996;Ohno et al., 1995). Only the form with a compromised tyrosine-motif binding pocket failed to associate with the peptide.

We also tested the influence of a set of mutations in the DEP domain on its association of Dvl2(417–588) with μ2C and with intact AP-2, purified from bovine brain (Fig. 6). Because the DEP-μ2 contact is weak, we chose to use as bait in the pull-down assay the Dvl2 fragment (417–588) containing both the DEP domain and the tyrosine motif. We therefore were testing for modulations in apparent affinity, rather than all-or-none effects. Mutating the tyrosine residue of YHEL results in a substantial loss of binding as expected (Yu et al., 2007). Single polar amino-acid changes (Asp441Lys, Asn451Ala, Arg489Ala) reduced affinity; double or triple mutation did not produce a further decrease (Fig. 6). We conclude that even the single substitutions in the DEP domain fully destabilize the DEP:μ2 interface, and further changes do not affect the basal affinity determined by the tyrosine motif.

(The K to M mutation in the DEP domain corresponding to the dsh^1allele in fruit flies first defined the PCP pathway (Axelrod et al., 1998). Two additional mutations, Lys446Ala and Lys446Met, at a position near the DEP:μ2 interface, but not part of a direct contact, also influence μ2 affinity (roughly a twofold decrease, data not shown). Position 446 is at the tip of the β1′-β2′ ribbon, which appears to have alternative possible conformations (see comparison of the conformation of this loop in the complex with μ2C and in the solution structure of the DEP domain alone). Substitutions at the tip of the ribbon could influence its conformational preferences and thus affect the association of the domain with μ2C. For example, a very small change in the conformation of the β1′-β2′ turn would allow Lys446 to form a salt bridge with Asp417 on μ2.

Effect of mutations on endocytosis of Frizzled

We took advantage of the mutational analysis just described to test whether the observed interface between μ2 and DEP is indeed critical for Frizzled internalization. For this purpose, we followed a method that we had developed previously to identify proteins participating in endocytosis of Fz4 (Yu et al., 2007). We expressed HA-tagged Fz4 and

NIH-PA Author Manuscript

NIH-PA Author Manuscript

NIH-PA Author Manuscript

Myc-tagged Dvl2 in HEK293T cells and monitored internalization and degradation of the HA-Fz4 by following uptake of an anti-HA antibody added to the medium immediately before adding Wnt and PMA.

As shown in Fig. 7, treatment with Wnt5A and PMA for 20 min stimulates uptake of Fz4, as indicated by the punctate distribution of anti-HA within cells co-expressing wild-type Dvl2. Note that in cells with complete Frizzled endocytosis, Dvl2 separates from Fz4 following uptake (Figs. 7A and B, Dvl2 YHEL). As reported in our earlier paper (Yu et al., 2007), a point mutation in the YHEL motif of Dvl2 blocked internalization of HA-Fz4 (Figs. 7A and B, Dvl2 AHEA), as did expression of Dvl2 K446M (Figs. 7A and B, Dvl2 K446M); the latter mutant is the equivalent of K417M in *Drosophila* Dsh, the original *dsh*^{1} allele identified with a defect in non-canonical Wnt signaling (Axelrod et al., 1998;Boutros et al., 2000;Perrimon and Mahowald, 1987). Expression of Dvl2 D441K,N451A,R489A -- a triple mutant combining the three interface mutations characterized in the experiments shown in Fig. 6 -- allowed a limited level of internalization following treatment with Wnt5A and PMA (Figs. 7A and B, Dvl2 D441K,N451A,R489A), but substantially less than expression of wild-type Dvl2. The relative strengths of the AHEA and D441K,N451A,R489A mutant phenotypes correspond to their relative effects on μ2 binding. The tyrosine-motif mutation, which eliminates detectable association of Dvl2 and μ2C *in vitro*, completely disables endocytosis of Fz4; the triple mutation at the DEP-domain:μ2C interface has a partial effect.

Like wild-type Dvl2, the Dvl2 AHEA and D441K,N451A,R489A mutants relocate to the cell periphery when Fz4 is overexpressed, even without addition of Wnt5A/PMA. Dvl2 K446M does not. This observation agrees with previous reports that the K446M mutation in the DEP domain prevents membrane recruitment of Dvl2 and suggests that modifications at the tip of the β1′-β2′ ribbon affect an earlier step in Frizzled endocytosis than the one affected by alterations in the surface containing Asp441, Asn451 and Arg489.

Discussion

The structure of the Dvl2:μ2C complex just described shows specific features of the bipartite interaction inferred from our earlier work. One component of the contact is the familiar tyrosine-motif interaction, essentially the same as those analyzed previously (Boll et al., 1996; Modis et al., 2001; Ohno et al., 1995; Owen and Evans, 1998). Like all the cargo-adaptor interactions in structures so far determined, this contact is a “peptide-domain” association, with a short motif on an unfolded segment of the cargo polypeptide chain inserted into a surface binding site on a well-folded domain of the adaptor subunit (Fig. 4). The other component of the Dvl2:μ2C contact is a new “domain-domain” interface, with complementary surfaces of two folded structures docked against each other.

The interaction between the DEP domain and μ2C helps resolve a puzzle posed by the contrast between the very extensive surface presented by μ2C and the extremely restricted patch dedicated to recognition of the tyrosine motif. The DEP interface now shows that a part of the exposed μ2C surface distinct from the tyrosine-motif site participates in cargo binding. The result suggests that other parts of that surface may also have partners, as yet unidentified. The incorporation of two interaction modes into one cargo molecule further suggests that combinatorial recognition (and combinatorial cargo addressing) may likewise be more widespread than hitherto suspected.

Frizzled recruits Dishevelled to the plasma membrane, in part through an interaction between a KTxxxW motif at the Frizzled C-terminus and a Dishevelled PDZ domain (Punchihewa et al., 2009; Zhang et al., 2009). The recruitment, which is Wnt independent, also requires the DEP domain. The product of the dsh^{1}(K446M) allele has a defect in this

NIH-PA Author Manuscript

NIH-PA Author Manuscript

NIH-PA Author Manuscript

translocation (Axelrod et al., 1998). Some recently published work suggests that a positively-charged patch containing lysines 477 and 484 in the DEP domain contributes to membrane recruitment of Dishevelled, perhaps through interaction with negatively charged lipid headgroups (Simons et al., 2009). These residues are not in the contact with μ2C in the crystal structure, and we have shown that mutation to glutamic acid of Lys477 and Lys484 in the DEP domain of Dvl2 does not affect the Dvl2:μ2 interaction (data not shown). The superposition in Fig. 4 shows that when Dvl2 binds AP-2, the surface of the DEP domain that bears these lysine residues faces in the same direction as does the site on the α-chain of the AP-2 core that binds phosphatidylinositol-4,5-bisphosphate (Collins et al., 2002). The two interactions could occur together on a roughly planar lipid bilayer if the μ2C domain were to rock slightly out of its position in the unliganded AP-2 complex (as it must do, to open up the tyrosine-motif site). Lys446 does not lie in the same plane, however, and if the DEP domain were oriented to present lysines 477 and 484 to lipid headgroups, Lys446 would be displaced by about 35 Å from the lipid bilayer surface. The loss of membrane recruitment when this residue is changed to Met would therefore need to come from disruption of some other contact. A cytoplasmic segment of Fz4 is the most likely candidate for this additional contact, because the Lys446Met mutation eliminates even the Wnt-independent (and hence AP-2 independent) membrane recruitment of Dvl2 by Fz4.

Uptake of the Frizzled:Dishevelled complex appears to require conformational changes in Frizzled. Transient expression of the two proteins leads to membrane recruitment of Dishevelled, but endocytosis requires Wnt. One possibility is that unliganded Frizzled interferes with the DEP-domain:μ2 contact seen in our structure and that activation by Wnt relieves this inhibition (Punchihewa et al., 2009). There is evidence for direct DEP domain:seven transmembrane-protein contact in other contexts (Ballon et al., 2006). Frizzled might also contact μ2 directly, as Dvl2 Lys446 (the site of the potential Frizzled contact just proposed) is adjacent to the μ2 interface.

If internalization of Frizzled is an immediate result of Wnt binding, signaling from the non-canonical branch of the Wnt pathway may occur in early endosomes, after uptake of the activated receptor, rather than only at the cell surface. Recent work suggests that Rac1, a downstream component of the non-canonical Wnt signaling pathway, is activated on the surface of early endosomes by recruitment of the Rac1-specific GEF Tiam1 (Palamidessi et al., 2008). The interaction documented here couples the Wnt-activated Dishevelled-Frizzled complex to the machinery likely to bring it into the appropriate endosomal compartment.

Materials and Methods

Reagents, clones, and constructs

Cell lines, reagents and antibodies have been described previously {yu, 2007}. Plasmids encoding HA-Fz4, Myc-Dvl2, GST-TGN38-YQRL have also been described {yu, 2007, Werner traffic paper, Banifacino paper}. Plasmids encoding the GST-tagged Dvl2 417–588 and μ2 170–435 (μ2C) were generated using the pGEX-4T1 bacterial expression vector. Plasmids expressing His-tagged Dvl2 407–588 and μ2C were generated using the pPROEX-HTC bacterial expression vector. Multiple point mutations in the specific constructs were introduced using the QuickChange protocol (Stratagene). To construct the plasmid expressing the chimeric protein, cDNA encoding the fragment of Dvl2 from residue 407 to 571 was cloned into pPROEX-HTC plasmid following the His tag and the TEV protease cleavage site. Two Sac II cleavage sites were inserted after residues 511 and 559 using the QuickChange protocol. The region between the added Sac II sites was removed by Sac II digestion and re-ligation. The C-terminal domain of μ2 adaptin (μ2C) was amplified with a forward primer with a overhanging region encoding EcoRI site followed by a Gly-Gly-Ser-Gly-Gly-Ser linker and a reverse primer encoding an Xho I site and the C-terminal end of μ2

NIH-PA Author Manuscript

NIH-PA Author Manuscript

NIH-PA Author Manuscript

adaptin. The PCR fragment was digested and inserted into the proEXHTC-Dvl2 407–571 plasmid with the internal deletion. The resulting construct expresses a protein containing the DEP domain of Dvl2 (407–510), a shortened 11-residue intra-molecular loop, the YHEL motif, a GGSGGS linker, and the C-terminal domain of μ2 adaptin (μ2C).

Expression, purification, and crystallization of the Dvl2:μ2C chimera

The recombinant His-tagged protein with a TEV cleavage site following the tag was expressed in E. coli at 16 °C. The protein was purified by passage over a Ni-NTA resin (GE Healthcare Life Sciences), then subjected to TEV cleavage. The de-tagged protein was further purified by chromatography on SP-Sepharose HP followed by gel filtration on S200 (GE Healthcare Life Sciences). The final concentration was 20 mg/mL in 20 mM Hepes at pH 7.5, 0.5 M NaCl, and 2 mM dithiothreitol (DTT). Single crystals (typical size 0.3mm × 0.2mm × 0.2mm) were obtained with hanging-drop vapor diffusion at 20°C by mixing 1 μL of the protein solution and 1 μL of the reservoir solution (0.7 M K/Na tartrate, 0.1 M sodium citrate, pH 5.5,10 mM DTT). Cryo-protection for x-ray data collection in a boiling nitrogen stream was in 25% glycerol.

Data collection and structure determination

Diffraction data were collected at the Advanced Photon Source, beamline 24-ID-E, and processed and scaled with HKL2000 (Otwinowski and Minor, 1997). Data to a minimum Bragg spacing of 3.5 Å were used for structure determination and refinement (Table 1). The structure was determined by molecular replacement using the program Phaser. The C-terminal domain of a murine μ2 adaptin subunit (PDB entry 1BW8) and a DEP domain (PDB entry 1FSH) were used as search models. Maps were inspected and models modified with the program Coot. The model coordinates were refined with CNS (Brunger et al., 1998). A test set containing 5% of all reflections was used throughout the refinement. The inter-molecular linker was built, and the DEP domain rebuilt, after the first round of rigid body refinement, positional refinement, and density modification with 6-fold n.c.s averaging. Linker connectivity's were unambiguous. Well ordered density was present in the initial, molecular-replacement density map for the linker that bridges μ2C R170 and the tyrosine motif bound to μ2C of an adjacent molecule. Scattered density appeared after a few cycles of refinement between the tyrosine motif and the C-terminus of the DEP domain associated with the μ2C covalently linked to that tyrosine motif. The model was further refined and rebuilt until the R factors ceased to drop. The stereochemistry of the models was monitored using Molprobity (Davis et al., 2007). Structural superposition was performed using LSQMAN from Uppsala Software Factory. Pymol was used to generate figures in this paper. Coordinates have been deposited in the Protein Data Bank (PDB ID: 3ML6).

In vitro GST pull-down

Purified GST-tagged proteins (~2 μg) were adsorbed to 7.5 μl glutathione beads in 20mM Hepes (pH7.5), 250 mM NaCl, 1 mM EDTA, 1 mM DTT. Purified proteins (AP-2, His-tagged Dvl2 407–588 and His-tagged μ2C) at final concentrations of 2.5, 15 and 1 μg/ml were incubated with immobilized GST-tagged proteins for 1 h at 4°C in 200 μl buffer containing 0.2 mg/ml BSA, 100 mM MES (pH 7.0), 150 mM KCl, 1 mM EDTA, 1mM DTT and 1% Triton-X-100. The beads were washed three times with the same buffer. Bound proteins were analyzed by SDS-PAGE and western blotting. The data represent the results obtained from three or four independent experiments.

Internalization assay

Internalization of HA-Fz4 in HEK293T cells expressing different Myc-Dvl2 proteins was stimulated with Wnt5A-conditioned medium in the presence of 1 μM PMA for 20 min as

NIH-PA Author Manuscript

NIH-PA Author Manuscript

NIH-PA Author Manuscript

described previously (Yu et al., 2007). Images were acquired using a Marianas™ system (Intelligent Imaging Innovations, Denver, CO) equiped with inverted microscope (Zeiss, Axio-Observer using a Plan-Apo 63x 1.4 NA objective), a Yokogawa spinning disk confocal unit (model CSU-22), a computer-controlled spherical aberration correction unit (Intelligent Imaging Innovations) and a Photometrics Cascade EM CCD camera. All the hardware was controlled by SlideBook version 4.2 (Intelligent Imaging Innovations). Single focal planes are shown approximately centered in the middle of the cell. Representative images correspond to data obtained from two independent experiments and more than 300 cells.

Supplementary Material

Refer to Web version on PubMed Central for supplementary material.

Acknowledgments

We thank the staff of the Northeast Collaborative Access Team at the Advanced Photon Source for assistance with x-ray diffraction data collection, Kevin Corbett for collecting diffraction data, Iris Rapoport, Werner Boll, Till Böcking for AP-2 preparations and Eric Marino for maintaining the fluorescence microscopy resource. The research was supported by NIH grant GM36548, 075252 and U54 AI057159 (NERCE Imaging Resource) (to TK). YX acknowledges a Ruth Kirschstein National Research Service Award. SCH is an Investigator in the Howard Hughes Medical Institute.

References

Axelrod JD, Miller JR, Shulman JM, Moon RT, Perrimon N. Differential recruitment of Dishevelled provides signaling specificity in the planar cell polarity and Wingless signaling pathways. Genes Dev. 1998; 12:2610–2622. [PubMed: 9716412]

Ballon DR, Flanary PL, Gladue DP, Konopka JB, Dohlman HG, Thorner J. DEP-domain-mediated regulation of GPCR signaling responses. Cell. 2006; 126:1079–1093. [PubMed: 16990133]

Blitzer JT, Nusse R. A critical role for endocytosis in Wnt signaling. BMC cell biology. 2006; 7:28. [PubMed: 16824228]

Boll W, Ohno H, Songyang Z, Rapoport I, Cantley LC, Bonifacino JS, Kirchhausen T. Sequence requirements for the recognition of tyrosine-based endocytic signals by clathrin AP-2 complexes. EMBO J. 1996; 15:5789–5795. [PubMed: 8918456]

Boutros M, Mihaly J, Bouwmeester T, Mlodzik M. Signaling specificity by Frizzled receptors in Drosophila. Science. 2000; 288:1825–1828. [PubMed: 10846164]

Boutros M, Mlodzik M. Dishevelled: at the crossroads of divergent intracellular signaling pathways. Mech Dev. 1999; 83:27–37. [PubMed: 10507837]

Chen W, ten Berge D, Brown J, Ahn S, Hu LA, Miller WE, Caron MG, Barak LS, Nusse R, Lefkowitz RJ. Dishevelled 2 recruits beta-arrestin 2 to mediate Wnt5A-stimulated endocytosis of Frizzled 4. Science. 2003; 301:1391–1394. [PubMed: 12958364]

Collins BM, McCoy AJ, Kent HM, Evans PR, Owen DJ. Molecular architecture and functional model of the endocytic AP2 complex. Cell. 2002; 109:523–535. [PubMed: 12086608]

Davis IW, Leaver-Fay A, Chen VB, Block JN, Kapral GJ, Wang X, Murray LW, Arendall WB 3rd, Snoeyink J, Richardson JS, et al. MolProbity: all-atom contacts and structure validation for proteins and nucleic acids. Nucleic acids research. 2007; 35:W375–383. [PubMed: 17452350]

Dubois L, Lecourtois M, Alexandre C, Hirst E, Vincent JP. Regulated endocytic routing modulates wingless signaling in Drosophila embryos. Cell. 2001; 105:613–624. [PubMed: 11389831]

Eaton S, Simons K. Apical, basal, and lateral cues for epithelial polarization. Cell. 1995; 82:5–8. [PubMed: 7606785]

Fanto M, Weber U, Strutt DI, Mlodzik M. Nuclear signaling by Rac and Rho GTPases is required in the establishment of epithelial planar polarity in the Drosophila eye. Curr Biol. 2000; 10:979–988. [PubMed: 10985385]

NIH-PA Author Manuscript

NIH-PA Author Manuscript

NIH-PA Author Manuscript

He X, Semenov M, Tamai K, Zeng X. LDL receptor-related proteins 5 and 6 in Wnt/beta-catenin signaling: arrows point the way. Development. 2004; 131:1663–1677. [PubMed: 15084453]

Kikuchi A, Yamamoto H, Sato A. Selective activation mechanisms of Wnt signaling pathways. Trends Cell Biol. 2009; 19:119–129. [PubMed: 19208479]

Kirchhausen T. Adaptors for clathrin mediated traffic. Annu Rev Cell Dev Biol. 1999; 15:705–732. [PubMed: 10611976]

Logan CY, Nusse R. The Wnt signaling pathway in development and disease. Annu Rev Cell Dev Biol. 2004; 20:781–810. [PubMed: 15473860]

Modis Y, Boll W, Rapoport I, Kirchhausen T. μ2-adaptin Subunit (AP50) Of AP-2 Clathrin Adaptor, Complexed With EGFR Internalization Peptide FYRALM At 2.5 Å Resolution. PDB entry. 2001:1131.

Ohno H, Stewart J, Fournier MC, Bosshart H, Rhee I, Miyatake S, Saito T, Gallusser A, Kirchhausen T, Bonifacino JS. Interaction of tyrosine-based sorting signals with clathrin-associated proteins. Science. 1995; 269:1872–1875. [PubMed: 7569928]

Owen DJ, Collins BM, Evans PR. Adaptors for clathrin coats: structure and function. Annu Rev Cell Dev Biol. 2004; 20:153–191. [PubMed: 15473838]

Owen DJ, Evans PR. A Structural Explanation For the Recognition of Tyrosine-Based Endocytotic Signals. Science. 1998; 282:1327–1332. [PubMed: 9812899]

Palamidessi A, Frittoli E, Garre M, Faretta M, Mione M, Testa I, Diaspro A, Lanzetti L, Scita G, Di Fiore PP. Endocytic trafficking of Rac is required for the spatial restriction of signaling in cell migration. Cell. 2008; 134:135–147. [PubMed: 18614017]

Perrimon N, Mahowald AP. Multiple functions of segment polarity genes in Drosophila. Dev Biol. 1987; 119:587–600. [PubMed: 3803719]

Piddini E, Marshall F, Dubois L, Hirst E, Vincent JP. Arrow (LRP6) and Frizzled2 cooperate to degrade Wingless in Drosophila imaginal discs. Development. 2005; 132:5479–5489. [PubMed: 16291792]

Punchihewa C, Ferreira AM, Cassell R, Rodrigues P, Fujii N. Sequence requirement and subtype specificity in the high-affinity interaction between human frizzled and dishevelled proteins. Protein Sci. 2009; 18:994–1002. [PubMed: 19388021]

Rives AF, Rochlin KM, Wehrli M, Schwartz SL, DiNardo S. Endocytic trafficking of Wingless and its receptors, Arrow and DFrizzled-2, in the Drosophila wing. Dev Biol. 2006; 293:268–283. [PubMed: 16530179]

Sato A, Yamamoto H, Sakane H, Koyama H, Kikuchi A. Wnt5a regulates distinct signalling pathways by binding to Frizzled2. Embo J. 2010; 29:41–54. [PubMed: 19910923]

Seto ES, Bellen HJ. Internalization is required for proper Wingless signaling in Drosophila melanogaster. J Cell Biol. 2006; 173:95–106. [PubMed: 16606693]

Simons M, Gault WJ, Gotthardt D, Rohatgi R, Klein TJ, Shao Y, Lee HJ, Wu AL, Fang Y, Satlin LM, et al. Electrochemical cues regulate assembly of the Frizzled/Dishevelled complex at the plasma membrane during planar epithelial polarization. Nat Cell Biol. 2009; 11:286–294. [PubMed: 19234454]

Tamai K, Semenov M, Kato Y, Spokony R, Liu C, Katsuyama Y, Hess F, Saint-Jeannet JP, He X. LDL-receptor-related proteins in Wnt signal transduction. Nature. 2000; 407:530–535. [PubMed: 11029007]

Veeman MT, Axelrod JD, Moon RT. A second canon. Functions and mechanisms of beta-catenin-independent Wnt signaling. Dev Cell. 2003; 5:367–377. [PubMed: 12967557]

Wallingford JB, Habas R. The developmental biology of Dishevelled: an enigmatic protein governing cell fate and cell polarity. Development. 2005; 132:4421–4436. [PubMed: 16192308]

Wehrli M, Dougan ST, Caldwell K, O'Keefe L, Schwartz S, Vaizel-Ohayon D, Schejter E, Tomlinson A, DiNardo S. arrow encodes an LDL-receptor-related protein essential for Wingless signalling. Nature. 2000; 407:527–530. [PubMed: 11029006]

Wehrli M, Tomlinson A. Independent regulation of anterior/posterior and equatorial/polar polarity in the Drosophila eye; evidence for the involvement of Wnt signaling in the equatorial/polar axis. Development. 1998; 125:1421–1432. [PubMed: 9502723]

NIH-PA Author Manuscript

NIH-PA Author Manuscript

NIH-PA Author Manuscript

Wong HC, Mao J, Nguyen JT, Srinivas S, Zhang W, Liu B, Li L, Wu D, Zheng J. Structural basis of the recognition of the dishevelled DEP domain in the Wnt signaling pathway. Nat Struct Biol. 2000; 7:1178–1184. [PubMed: 11101902]

Yu A, Rual JF, Tamai K, Harada Y, Vidal M, He X, Kirchhausen T. Association of Dishevelled with the clathrin AP-2 adaptor is required for Frizzled endocytosis and planar cell polarity signaling. Dev Cell. 2007; 12:129–141. [PubMed: 17199046]

Zhang Y, Appleton BA, Wiesmann C, Lau T, Costa M, Hannoush RN, Sidhu SS. Inhibition of Wnt signaling by Dishevelled PDZ peptides. Nat Chem Biol. 2009; 5:217–219. [PubMed: 19252499]

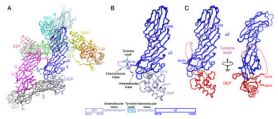

Figure 1. Structure of the Dvl2:μ2 complex

(A) Crystal packing in one asymmetric unit, showing the “domain swap” of the tyorine-motif segment. Each polypeptide chain is in a single color range, with the DEP domain much lighter than μ2. In the foreground are two polypeptide chains, in blue (DEP is silver-blue; μ2 is strong blue; tyrosine motif has an intermediate shade) and magenta (DEP is pink; μ2 is strong magenta; tyrosine motif is an intermediate red). These two chains swap tyrosine-motif segments, so that the blue tyrosine motif binds the receiving site on the magenta μ2 and vice-versa. (B) Domain organization of the “blue” chimera. (C) A composite structure of the DEP domain (red) and the tyrosine motif (pink) of Dvl2 bound to the C-terminal region of μ2 (μ2C) (blue).

NIH-PA Author Manuscript NIH-PA Author Manuscript NIH-PA Author Manuscript

NIH-PA Author Manuscript
NIH-PA Author Manuscript
NIH-PA Author Manuscript

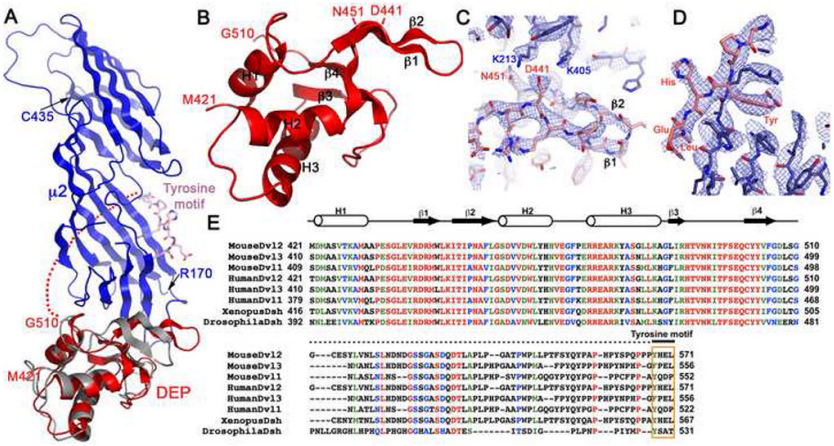

Figure 2. The Dvl2 DEP domain

(A) Superposition of the Dvl2 DEP domain from an NMR solution structure (grey) (Wong et al, 2000) onto the Dvl2:μ2 crystal structure (colored as in Fig 1B). (B) The structure of the DEP domain with secondary structure elements labeled. (C) The 2Fo-Fc map at 2σ in the β1–β2 loop region of the DEP domain. Residues from μ2 and DEP domain are colored in red and blue respectively. (D) Sequence alignment of Dishevelled proteins, generated by ClustalW and manually modified. Residues colored red, green, blue and black are identical, with strong similarity, weak similarity and different, respectively.

NIH-PA Author Manuscript

NIH-PA Author Manuscript

NIH-PA Author Manuscript

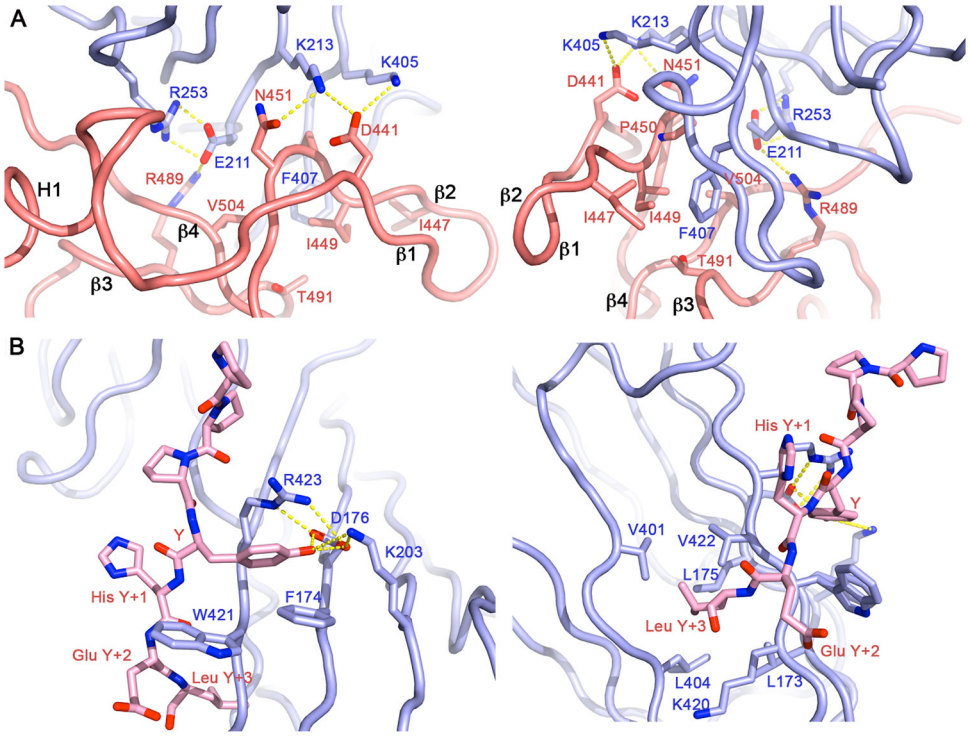

Figure 3. Dvl2:μ2 interface

(A) Interface of DEP domain and μ2. (B) Interface of YHEL Tyrosine motif and μ2. Salt bridges and H-bonds are shown as yellow dashed lines. Left panels show hydrophilic interactions; right panels, viewed from the opposite side, show hydrophobic interactions. Molecular models colored as in Fig 1C.

NIH-PA Author Manuscript

NIH-PA Author Manuscript

NIH-PA Author Manuscript

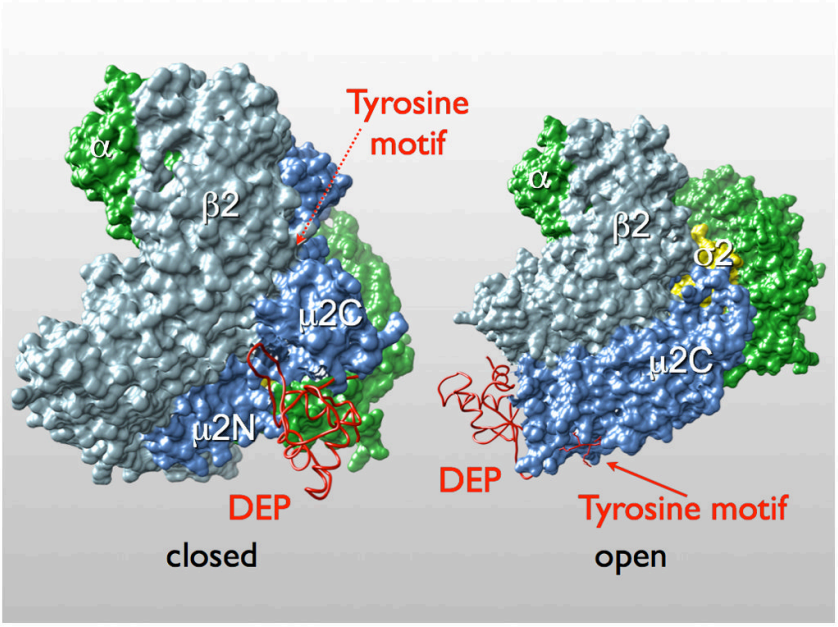

Figure 4. Superposition of Dvl2:μ2 complex on the AP-2 clathrin adaptor core

Locations of known endocytic motifs and lipid binding site are marked. The AP-2 core structure is shown as a surface rendering (α chain in green; β2 in light blue; μ2 in blue; σ2 in yellow) and the Dvl2 DEP domain in worm representation (red).

NIH-PA Author Manuscript
NIH-PA Author Manuscript
NIH-PA Author Manuscript

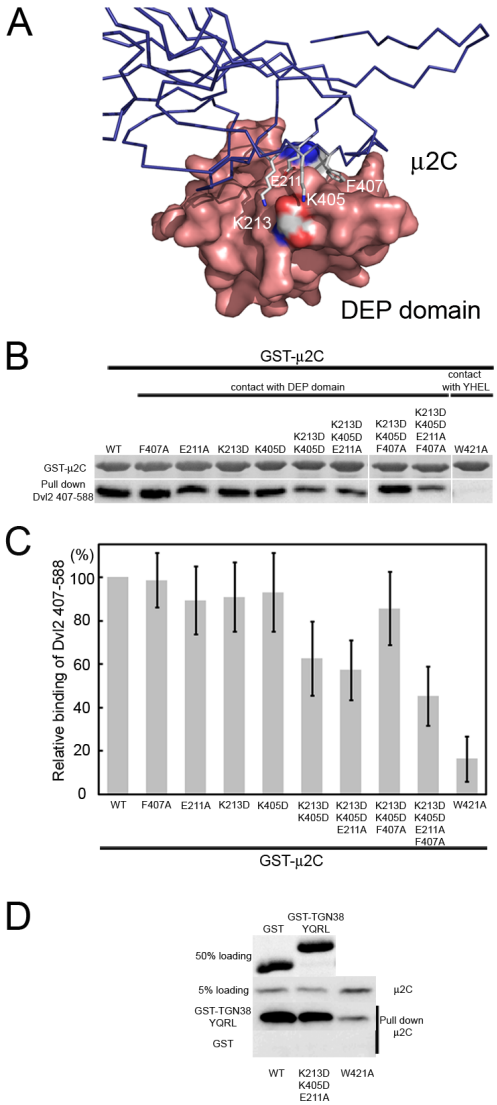

Figure 5. Influence of specific mutations in μ2 on its association with the DEP domain of Dvl2

(A) Schematic representation of the Dvl2:μ2 interface; μ2C (blue) is represented as a ribbon diagram; DEP domain (pink), as a surface rendering. Residues E211, K213, K405 and F407 of μ2C, that make close contacts with the DEP domain of Dishevelled 2 are highlighted. (B) Pull-down assay with bacterially expressed wild-type or point-mutant μ2C fused to GST and His-tagged Dvl2 407–588. Bound GST-containing proteins were detected by SDS-PAGE followed by Coomassie Blue staining (50% input). Bound Dvl2 407–588 proteins were detected from a second sample processed identically, by western blot analysis with the antibody specific for the His tag in Dvl2 407–588 (50% input). The results are representative of four independent experiments. (C) Relative binding of Dvl2 407–588 to the GST-μ2C wild type and mutants used in panel B. The binding of the wild-type μ2C was set as 100%. Data correspond to average +/− std from four experiments. (D) Pull-down assay with a short peptide containing the YQRL sorting motif from TGN38 fused to GST and His-tagged Dvl2 407–588. Bound GST-containing proteins were detected by SDS-PAGE followed by Coomassie Blue staining (50% input). Bound μ2C was detected from a second sample processed identically, by western blot analysis with the antibody specific for the His tag in μ2C (50% input). The results are representative of three independent experiments.

NIH-PA Author Manuscript

NIH-PA Author Manuscript

NIH-PA Author Manuscript

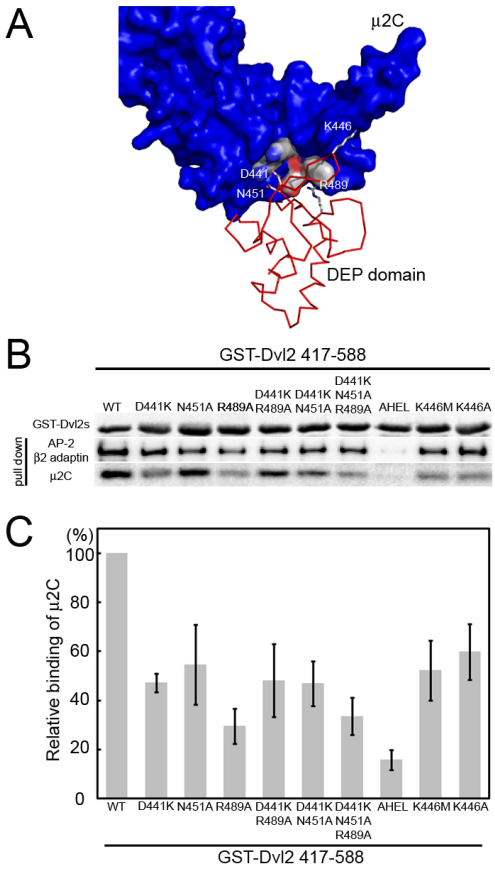

Figure 6. Influence of specific mutations in the DEP domain of Dvl2 on its association with μ2 or with the AP-2 clathrin adaptor

(A) Schematic representation of the Dvl2:μ2 interface; μ2C (blue) is represented as a surface rendering and the DEP domain (pink) is shown as a ribbon diagram. Residues D441, R489 and N451 of the DEP domain at the interface with μ2C are highlighted. K446 is also shown. (B) Pull-down assay with GST-Dvl2 417–588 and AP-2 clathrin adaptor purified from calf brain coated vesicles or recombinant μ2C. Bound GST-containing proteins were detected by SDS-PAGE followed by Coomassie Blue staining (50% input). Bound AP-2 or μ2C were detected from a second sample processed identically, by western blot analysis with the antibody specific for β!2-adaptins of AP-2 or with the antibody specific for the His tag for μ2C (50% input). The results are representative of three experiments. (C) Relative binding of μ2C to the GST-Dvl2 407–588 variants used in panel B. The binding of the wild-type μ2C was set as 100%. Data correspond to average +/− std from three independent experiments.

NIH-PA Author Manuscript
NIH-PA Author Manuscript
NIH-PA Author Manuscript

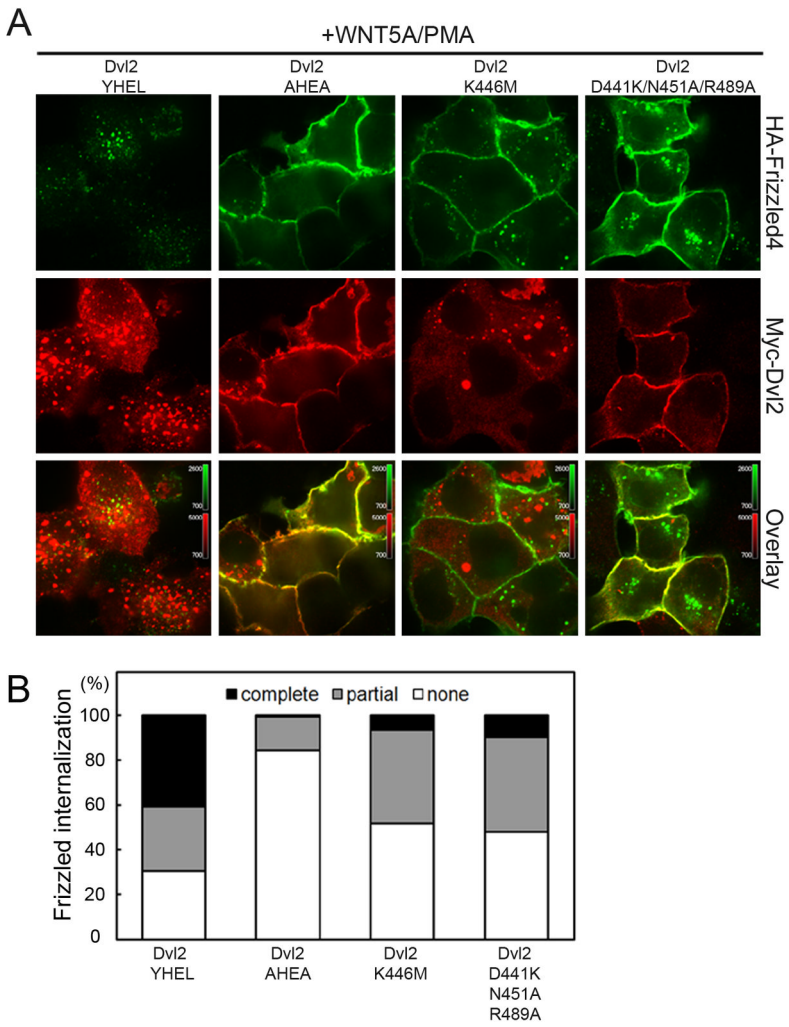

Figure 7. Effect of mutations in Dvl2 that interfere with AP-2 binding on internalization of activated Fz4

(A) HEK293T cells were cotransfected with plasmids encoding HA-Fz4 (green) together with Myc-tagged wild-type mouse Dvl2 bearing the YHEL sorting motif (Dvl2 YHEL, red), Myc-tagged Dishevelled2 with AHEA instead of the YHEL motif (Dvl2 AHEA, red), Myc-tagged Dishevelled2 with the K446M mutation in the DEP domain (Dvl2 K446M, red) or Myc-tagged Dishevelled2 with the triple mutation D441K, N451A and R489A in the DEP domain (Dvl2 D441K/N451A/R489A, red). After 24 h, cells were incubated at 37°C for 10 min with an antibody specific for the HA-epitope (green), then for 20 min, also at 37°C, c with fresh medium containing Wnt5A/PMA. Cells were fixed, permeabilized and processed for immunofluorescence. Representative examples from 15 independent fields from two independent experiments for each condition are shown using equal imaging settings.

(B) Analysis of images from fields corresponding to the experiments depicted in A. The extent of Fz4 internalization was scored in cells co-expressing Dvl2 and Fz4 according to previoiusly established criteria (Yu et al, 2007): (1) HA-Fz4 signal at the cell surface (none), (2) a mixture of HA-Fz4 signals at the cell surface together with a punctate intracellular pattern (partial) and (3) no discernable HA-Fz4 signal at the cell surface together with a weak intracellular punctate pattern (complete). About 300 cells were analyzed for each of the experimental conditions.

NIH-PA Author Manuscript
NIH-PA Author Manuscript
NIH-PA Author Manuscript

Table 1

Data collection and Refinement Statistics

Data Collection	
Space group	C2
Cell dimensions *a*,*b*,*c* (Å)	292.4, 98.1, 171.3,
β (°)	122.0
Resolution (Å)	100-3.5
R_{sym} (%)[1,2]	11.2 (77.4)
I/σ (I)[2]	11.3 (1.5)
Completeness (%)[2]	99.3 (97.0)
Redundancy[2]	3.6 (3.5)
Refinement	
Resolution (Å)	3.5
No. reflections	51395
R_{work}/R_{free} (%)[2]	30.8/33.5
R.m.s deviations	
Bond length (Å)	0.011
Bond angle (°)	1.4
Ramachandran analysis	
Favored/outlier (%)	87.6/0.0
Total residues	2006

[1] $R_{sym} = \Sigma\Sigma_j|I_j - \langle I\rangle|/\Sigma I_j$, where I_j is the intensity measurement for reflection j and $\langle I\rangle$ is the mean intensity for multiply recorded reflections.

[2] Values in parentheses are for the outermost resolution shell.

[3] $R_{work,\ free} = \Sigma||F_{obs}| - |F_{calc}||/|F_{obs}|$, where the working and free *R*-factors are calculated using the working and free reflection sets, respectively.